Proceedings World Geothermal Congress 2023
Beijing, China, April 17 – 21, 2023

Laboratory Study of Supercritical Carbon Dioxide Shock Fracturing in Hot Dry Rock

Xiaoguang Wu, Zhongwei Huang*, Zixiao Xie, Gensheng Li, Haizhu Wang, Wenchao Zou, Zhaowei Sun

State Key Laboratory of Petroleum Resources and Prospecting, China University of Petroleum, Beijing 102249, China

E-mail address, wuxg@cup.edu.cn; huangzw@cup.edu.cn

Keywords: Hot dry rock; Supercritical CO2; Fracturing; EGS; Geothermal stimulation

ABSTRACT

Hot dry rock (HDR) geothermal is a clean and renewable resource which presents a promising prospect in meeting the growing demand for energy and achieving low-carbon solutions. Creating an inter-connected and highly conductive fracture network is the foundation for obtaining enough heat transfer spaces and high flow flux of working fluid in HDR geothermal. However, the simple 2-D planar fracture pattern created by conventional water-based hydraulic fracturing could result in fast thermal breakthrough and shorten the life of Enhanced Geothermal System (EGS) significantly, and poses challenges for the environment due to the chemical additives and massive water consumption. Herein, a novel non-aqueous stimulation method is investigated, i.e. supercritical carbon dioxide shock (SCS) fracturing, which combines the advantages of supercritical CO2 (SC) fracturing and dynamic shock effect, providing potential solutions to the challenges above. To determine its stimulation performance in EGS, we performed controllable lab-scale SCS fracturing experiments on high-temperature granites subjected to true tri-axial stresses. By comparing with conventional water fracturing and SC-CO2 fracturing, the fracture initiation behavior and stimulation performance of SCS fracturing were investigated quantitatively based on CT scanning and reinjection tests, with respect to fracture morphology and conductivity. Effects of critical parameters were analyzed as well. Results indicate that the breakdown pressure of granite is 24.2~57.5% lower than the shock pressure during SCS fracturing, and it decreases with increasing rock temperature. SCS fracturing could create complex fracture network with more interconnected branches and larger seepage spaces. As compared to water fracturing and SC fracturing, the fracture conductivity of SCS fracturing is 3.4~7.0 times and 4.5~21.2 times higher, respectively. As the rock temperature increases, both the tortuosity and conductivity of fractures improve dramatically, which benefits to extend the flow path of working medium and enhance the heat transfer performance. In-situ stress plays a relatively weak role in controlling fracture propagation of SCS fracturing. At horizontal stress difference coefficient of 0.14~0.60, the fracture propagation behaves more randomly in direction, contributing to forming complex fractures with multi-branches. Higher shock pressure conduces to the stimulation performance enhancement of SCS fracturing, improving the complexity and connectivity of fracture networks, and promote the fracture to get rid of the control of in-situ stress in EGS. The key findings are expected to provide a novel insight into developing HDR geothermal in a more environmentally and more efficient way and achieving carbon storage and utilization.

1. INTRODUCTION

Geothermal energy is a renewable and sustainable resource which plays an important role in meeting the growing demand for energy and achieving low-carbon solutions (TESTER et al., 2006). Hot dry rock (HDR), as a typical type of geothermal resources, offers great potential of thermal energy. The HDR reservoir is characterized by the rocks with naturally low permeability and high temperature ranging from 150~650℃, located at 3~10 km depth below the earth's surface (RYBACH. L., 2010; HUENGES E., 2016). To enhance the permeability of HDR and extract geothermal quantities capable of producing electricity economically, hydraulic fracturing is generally employed to stimulate the reservoir and create pathways for working fluid flow and heat extraction between injection wells and production wells, also referred as enhanced geothermal system (EGS). In EGS, creating an inter-connected and highly conductive fracture network is the foundation for obtaining enough heat transfer spaces and high flow rates of working fluid in the reservoir. However, there are several challenges for conventional hydraulic fracturing in EGS, such as high breakdown pressure and simple fracture morphology. The lessons learned from previous EGS projects like Fenton Hill in US, Hijiori in Japan, Rosemanowes in England and etc. indicate that the simple 2-D planar fracture pattern created by conventional hydraulic fracturing is not desirable for HDR in most cases (POLLACK et al., 2020; OLASOLO et al., 2016), which could result in fast thermal breakthrough and shorten the service life of EGS significantly. Additionally, the conventional water-based fracturing fluid also poses challenges for the environment, due to the chemical additives and massive water consumption. Hence, finding a non-contamination and non-aqueous based fracturing method which could create 3-D complex inter-connected fracture networks, is the key to realize the effective stimulation of HDR and economic development of EGS.

To address issues above, the supercritical carbon dioxide (SC-CO2) shock fracturing was proposed to apply in the HDR geothermal stimulation. In this method, CO2 is used as an alternative to water-based fracturing fluid and injected into a specially designed downhole energizing device, in which the static pressure accumulates under the joint action of continuous injection and volume expansion of compressible fluid at high temperatures. Once the accumulated pressure exceeds the threshold value, the drainage channels of the downhole devices are opened to release controllable high-pressure shock waves instantly and crack the surrounding rocks, creating a volumetric fracture zone near wellbore. As the CO2 continues to be injected in the wellbore, these blasted fractures can be further expanded, forming a large-scale complex fracture network. Since the CO2 has a relatively low critical temperature and pressure (304.13K and 7.38 MPa), it keeps at supercritical state during the stimulation process of HDR.

The SC-CO2 shock fracturing, as a non-aqueous stimulation method, could offer potential solutions to the challenges mentioned above. This technique combines the advantages of SC-CO2 fracturing and dynamic shock effect. Firstly, SC-CO2 has the features of low viscosity and high permeability (Shi et al., 2019), which makes it easier to penetrate tight rocks and induce multi-branch fractures. When the dynamic shock wave induced by high-pressure blasting is coupled, the complexity and connectivity of the fracture networks can be further enhanced, improving the stimulation performance significantly. Next, the near-wellbore fracture zone induced by

blasting shock can effectively reduce the breakdown pressure and improve the injection capacity of EGS. Injection capacity is a key engineering parameter for EGS. A high injection capacity can significantly improve the heat extraction capacity in the reservoir. EGS could be considered as economical development only when the injection capacity reaches 50 kg/s. Finally, taking CO2 as the substitution of conventional water-based fracturing fluid can not only eliminate the environmental risks, but achieve CO2 storage and utilization, providing a potential decarbonization solution.

In fact, the stimulation enhancement mechanism of SC-CO2 shock fracturing is similar with CO2 blasting fracturing technique, which has already been widely used in mining, especially in the coalbed methane recovery. Priors implemented comprehensive investigations on the borehole pressure evolution, explosion energy, shock wave and fracture propagation of CO2 blasting fracturing experimentally and numerically (Cong et al., 2021; Chen et al., 2019; Ke et al., 2019; Shang et al., 2021; Shang et al., 2022; Wang et al., 2022; Hu et al., 2018; Hu et al., 2022). Field tests indicate that the quantity of gas extraction from a single borehole controlled by fracturing increased by about 4 times in the initial 8 hours after CO2 blasting (Wang et al., 2021). However, due to the relatively shallow burial depth of coal seam, CO2 exists in liquid phase rather than supercritical state during the fracturing process. As compared to liquid CO2, supercritical CO2 has very different physical properties, and thereby shows a great difference in the fracturing performance. Additionally, unlike coalbed methane formations, HDR is characterized by high-temperature in nature. Intense heat transfer and thermal stresses are involved in the dynamic blasting process. Previous literatures studied the fracturing performance and heat extraction capacity of CO2 in EGS, but the combined effect of thermal and blasting shock was rarely reported. Failure characteristics and fracture propagation patterns of rocks under the joint action of thermal stress and dynamic shock loading are still unclear.

To determine the stimulation performance and feasibility of SC-CO2 shock fracturing in EGS, we conducted controllable lab-scale SC-CO2 shock fracturing experiments on high-temperature granites subjected to true tri-axial stresses. Conventional water fracturing and SC-CO2 fracturing were also conducted as comparisons. Borehole pressure evolution was record and analyzed. The stimulation performances of the three fracturing methods were evaluated and contrasted, with respect to fracture morphology and conductivity. Effects of several critical parameters on the fracturing performance, such as shock pressure, tri-axial stress and rock temperature were investigated as well. The key findings are expected to provide a methodological and theoretical guidance for developing HDR geothermal in a more environmentally and more efficient way.

2. MATERIAL AND METHODS

2.1 Sample preparation

The rock material used in our experiments is granite collected from the Qiabuqia basin of Qinghai Province, which is a potential HDR project site in China. According to the X-ray diffraction (XRD) analysis as shown in Table 1, the granite is mainly composed of quartz (28.6%), K-feldspar (17.3%), plagioclase (42.9%) etc., in which the brittle materials occupy the majority. Basic mechanical properties of the granites were tested as well, as shown in Table 2. Before experiments, we cut the granites into cubes with the dimension of 100 mm in side length, as illustrated in Fig. 1. A centered hole with 16 mm in diameter and 60 mm in depth was drilled in the sample to simulate the wellbore. A stainless-steel casing extending 40 mm into the wellbore was cemented using the temperature resistant epoxy-resin adhesive, with a 20 mm open-hole section left. A piezometric sensor was set in the borehole to capture and record the pressure signals during the fracturing experiment, with the data acquisition rate of 1000 s^{-1}.

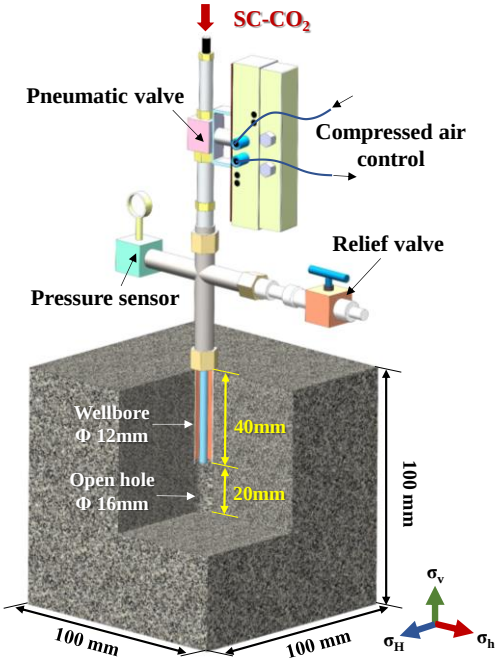

Fig. 1 Granite sample and wellbore setup.

Table 1 XRD test results of the mineral composition of granite.

Minerals	Quartz	K-feldspar	Plagioclase	Dolomite	Pyroxene	Clay minerals
Proportion	28.6%	17.3%	42.9%	2.3%	5.5%	3.4%

Table 2 Physical and mechanical properties of granite.

Properties	Density (kg/m^3)	Permeability (mD)	UCS (MPa)	Young's Modulus (GPa)	Poison's ratio	Tensile strength (MPa)
Values	2753±15	0.0069±0.001	153±10	34.2±2.1	0.19±0.08	10.3±0.08

2.2 Experimental setup and procedure

The lab-scale SC-CO2 shock fracturing in HDR is a complex process involving in generating a supercritical environment for the fracturing fluid and simulating the in-situ temperature and stress conditions of rocks simultaneously. In this work, a true triaxial SC-CO2 shock fracturing equipment of high-temperature rocks was designed and developed independently, as shown in Fig. 2 and Fig. 3, in which different stimulation experiments, such as SC-CO2 fracturing, SC-CO2 shock fracturing and water fracturing, can be carried out for rocks with different temperatures and stress. This equipment consists of five main modules, such as SC-CO2 generation, shock pressure control, true-triaxial stress loading, rock heating and temperature control, and data acquisition. The SC-CO2 generation, shock pressure control, triaxial loading module of high-temperature rocks are three unique modules differing from conventional triaxial fracturing experiment system.

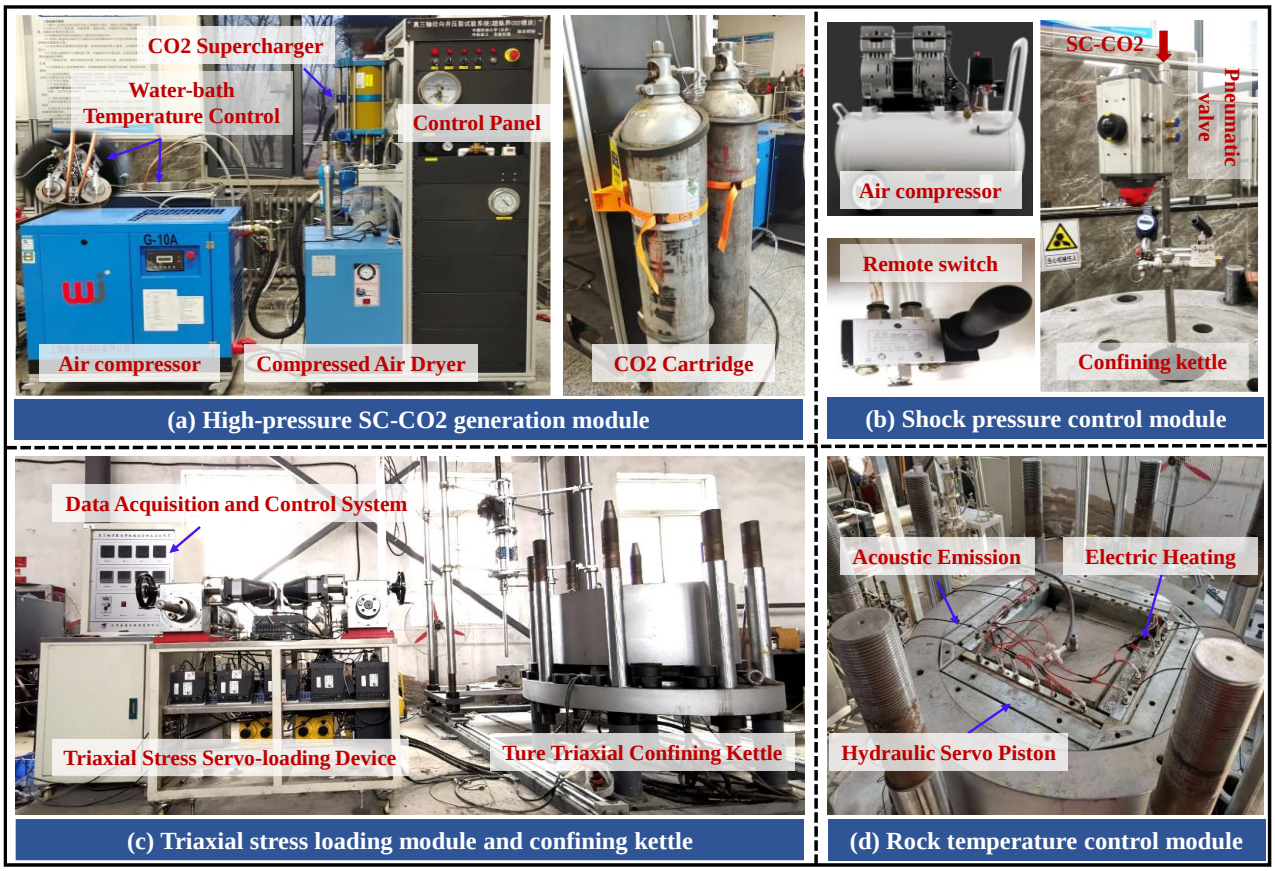

Fig. 2 Ture triaxial fracturing equipment for SC-CO2 shock in high-temperature rocks. (a) High-pressure SC-CO2 generation module; (b) Shock pressure control module; (c) Ture triaxial-loading module; (d) Rock temperature control in the confining kettle.

High-pressure SC-CO2 generation module (as shown in Fig. 2a). This module is designed to produce high-pressure SC-CO2 to pressurize the borehole. CO2 reaches the supercritical state when the pressure and temperature exceeds 7.38 MPa and 304.13 K, respectively. To simulate the supercritical environment, CO2 gas is pneumatically compressed by supercharger and then stored in an energy accumulation tank with a volume of 3000 mL. Fluid in this tank is heated by circulating water-bath, and temperature sensors are used to realize the feedback regulation and real-time control of the temperature. Maximum heating temperature of the fracturing fluid is 100℃.

Shock pressure control module. Unlike conventional hydraulic fracturing with stable and slow injection in the borehole, high-pressure SC-CO2 is released by the pneumatic valve into the borehole within milliseconds to induce shock waves and fractures. In this module, a screw air compressor is combined with the supercharger to energize the CO2 fluid with a pressurization ratio of 1:140, as shown in Fig. 2b. Max shock pressure of our device can reach 100 MPa.

True triaxial loading module of high-temperature rocks (as shown in Fig. 2c and 2d). This module is designed for the sample with the dimensions of 100~400 mm cubes. Triaxial stress up to 50 MPa can be loaded on the sample along x-axis, y-axis, and z-axis with an accuracy of ±0.1 MPa. To simulate the high-temperature conditions of HDR, 36 electric heating devices with a total power of 14.4 kW are uniformly arranged in the surrounding plate of triaxial loading unit, and temperature sensors are used to realize the monitoring of thermal loading and temperature feedback regulation of rock samples. The maximum heating rate can reach 100℃/h, but the maximum heating temperature generally does not exceed 200℃ for the safety of equipment. For the purpose of improving experimental efficiency, we preheated the rock samples to the target temperature in muffle furnace with a slow heating rate of 5℃ /min in this work, and then transfer to the triaxial stress loading unit for the temperature control.

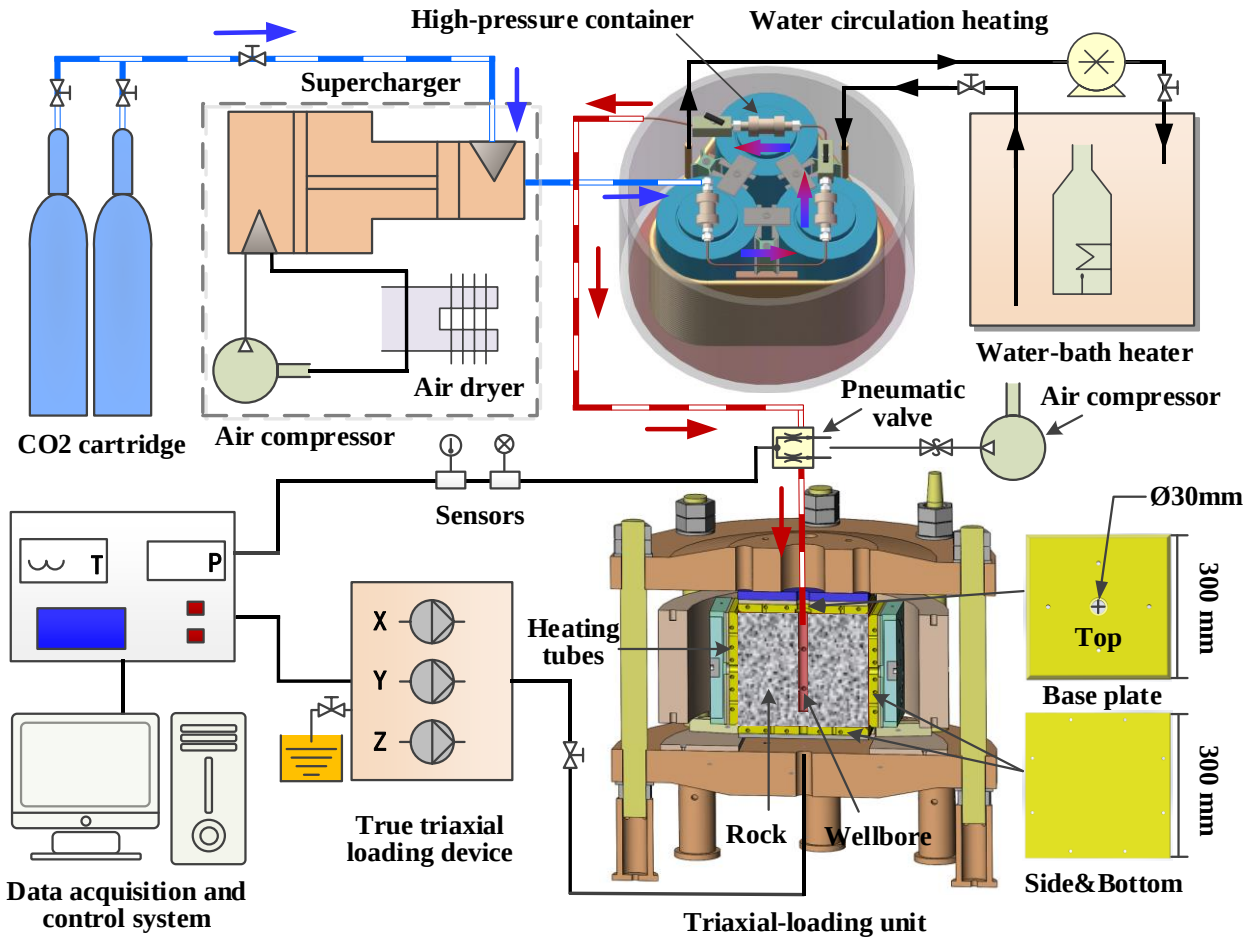

Fig. 3 Schematic of the true triaxial SC-CO2 shock fracturing system.

The procedure of SC-CO2 shock fracturing includes rock heating, triaxial stress loading, fluid pressurization, water-bath circulation heating and energy release for blasting, which are detailed as follows:

① Place the core that was slowly heated to the target temperature in advance in Muffle furnace quickly into the triaxial loading unit. A slow heating rate of 5℃/min was set for the furnace to prevent from thermal shock during heating;

② Heat the rock and control the temperature by using the electric heat tubes and thermocouples;

③ Turn on the true triaxial loading device, and load the triaxial stress according to the predetermined scheme;

④ Start the air compressor to drive the supercharger (gray dotted block in Fig. 3), and charge the CO2 from the cartridge into the high-pressure container and pressurize it (flow along the blue arrow in Fig. 3);

⑤ Turn on the water-bath heater to heat and control the temperature of high-pressure CO2 in the container by circulating water (flow along the black arrow in Fig. 3), and keep CO2 in the supercritical state, with the temperature of 60℃ and pressure ranging from 14 to 24MPa;

⑥ When the pressure of CO2 in the container reaches the predetermined value, the pneumatic valve can be remotely opened through the air compressor to realize the instantaneous release of high-pressure supercritical CO2 into the borehole (flow along the red arrow) and complete the stimulation of high-temperature rock sample. The data during the whole fracturing process such as temperature, pressure and triaxial stress can all be monitored by the data acquisition system;

⑦ Turn off the supercharge, water circulation pump and rock heating devices after experiments. Release the triaxial stresses and take out the rock sample for further analysis.

2.3 Experiment scheme

Table 3 shows the experiment scheme of this study. Totally 20 granite samples in 6 groups were tested under different triaxial stress and temperature conditions, with different fracturing methods. Samples in SCS 1-1~1-5, SCS 2-1~2-3, SCS 3-1~3-4 were used to perform the SC-CO2 shock fracturing tests on rocks with different temperatures (25~180 ℃) under the shock pressures of 14~24 MPa, while SCS 3-3, 4-1 and 4-2 were used to determine the effect of triaxial stress on the SC-CO2 shock fracturing. Three different tri-axial stress conditions were investigated, with the difference coefficient of horizontal stress ranging from 0.14 to 1.67. To better evaluate the performance of the SC-CO2 shock fracturing and identify its characteristics in fracture initiation and propagation, samples W-1~W-3 and SC-1~SC-3 were taken as comparisons in this study, to conduct water fracturing and conventional SC-CO2 fracturing on rocks with different temperatures. A constant injection rate of 10ml/min was applied in the water fracturing.

Table 3 Experimental matrix for water fracturing, SC-CO2 fracturing and SC-CO2 shock fracturing on high-temperature granite.

Sample No.	Fracturing type	Shock pressure Or Injection rates	$\sigma_H/\sigma_h/\sigma_v$ (MPa)	Granite temperature (℃)
SCS 1-1	SC-CO2 shock fracturing	14 MPa	8/5/10	25
SCS 1-2	SC-CO2 shock fracturing	16 MPa	8/5/10	25
SCS 1-3	SC-CO2 shock fracturing	18 MPa	8/5/10	25
SCS 1-4	SC-CO2 shock fracturing	20 MPa	8/5/10	25
SCS 1-5	SC-CO2 shock fracturing	24 MPa	8/5/10	25
SCS 2-1	SC-CO2 shock fracturing	16 MPa	8/5/10	100
SCS 2-2	SC-CO2 shock fracturing	20 MPa	8/5/10	100
SCS 2-3	SC-CO2 shock fracturing	24 MPa	8/5/10	100
SCS 3-1	SC-CO2 shock fracturing	16 MPa	8/5/10	180
SCS 3-2	SC-CO2 shock fracturing	18 MPa	8/5/10	180
SCS 3-3	SC-CO2 shock fracturing	20 MPa	8/5/10	180
SCS 3-4	SC-CO2 shock fracturing	24 MPa	8/5/10	180
SCS 4-1	SC-CO2 shock fracturing	20 MPa	8/3/10	180
SCS 4-2	SC-CO2 shock fracturing	20 MPa	8/7/10	180
W-1	Water fracturing	10 ml/min	8/5/10	25
W-2	Water fracturing	10 ml/min	8/5/10	100
W-3	Water fracturing	10 ml/min	8/5/10	180
SC-1	SC-CO2 fracturing	/	8/5/10	25
SC-2	SC-CO2 fracturing	/	8/5/10	100
SC-3	SC-CO2 fracturing	/	8/5/10	180

3. RESULTS AND ANALYSES

3.1 Pressure evolution in the wellbore

To determine the fracture initiation behaviors, we record the pressure in the borehole in real time during the fracturing process of different methods. The borehole pressure evolution curves of water fracturing, SC fracturing and SCS fracturing are plotted versus time in Fig. 4a, 4b and 4c, respectively. It is found that the borehole pressure of water fracturing increases gradually, followed by a sudden drop, indicating the initiation of fracture at the peak pressure (breakdown pressure), and then stabilized in a certain pressure value. Unlike water fracturing, SC fracturing presents a moderate pressure drop rate after the peak, which may be attributed to the relatively narrow fracture as compared to water fracturing. Note that high-pressure SC-CO2 was pushed by CO2, so that the pressurization of SC-CO2 started at a relatively high pressure.

The pressure evolution of SCS fracturing differs from that of water fracturing and SC fracturing greatly. In the SCS fracturing, the borehole pressure reaches to the peak rapidly in a few hundred milliseconds, applying a dynamic load in the wellbore, and then drops to 0MPa in a stepwise manner in several seconds. The whole fracturing period is less than 10 seconds, which is significantly shorter than those of water fracturing and SC fracturing. There are multiple short pressure plateaus in the curves due to the joint action of the pressure wave reflection and hedging in the borehole and the fracture propagation. Moreover, it is noted that the granite breaks at a peak pressure value that is 24.2~57.5% lower than the shock pressure during SCS fracturing. The rock temperature has a great influence on the breakdown pressure, as illustrated in Fig. 4d. The breakdown pressure decreases with increasing rock temperature for the three fracturing methods. As compared to the granite at 25℃, the breakdown pressure of granite at 180℃ reduces by 50.3%, 14.2% and 44.3% for water fracturing, SC fracturing and SCS fracturing, respectively. This fact is mainly attributed to the higher thermal stress induced by greater temperature difference between fracturing fluid and rocks, which facilitate the initiation of fractures. Among the three fracturing methods, SC fracturing has the lowest breakdown pressure for granite samples with the same temperature, substantiating that the low-viscosity and low-density supercritical fluid benefits to lower the breakdown pressure of granite. Although the working medium for both SC fracturing and SCS fracturing is supercritical fluid, the heat transfer and corresponding thermal stress in the SCS fracturing are weaker than those in SC fracturing due to the short fracturing period, thereby leading to a relatively higher breakdown pressure in SCS fracturing.

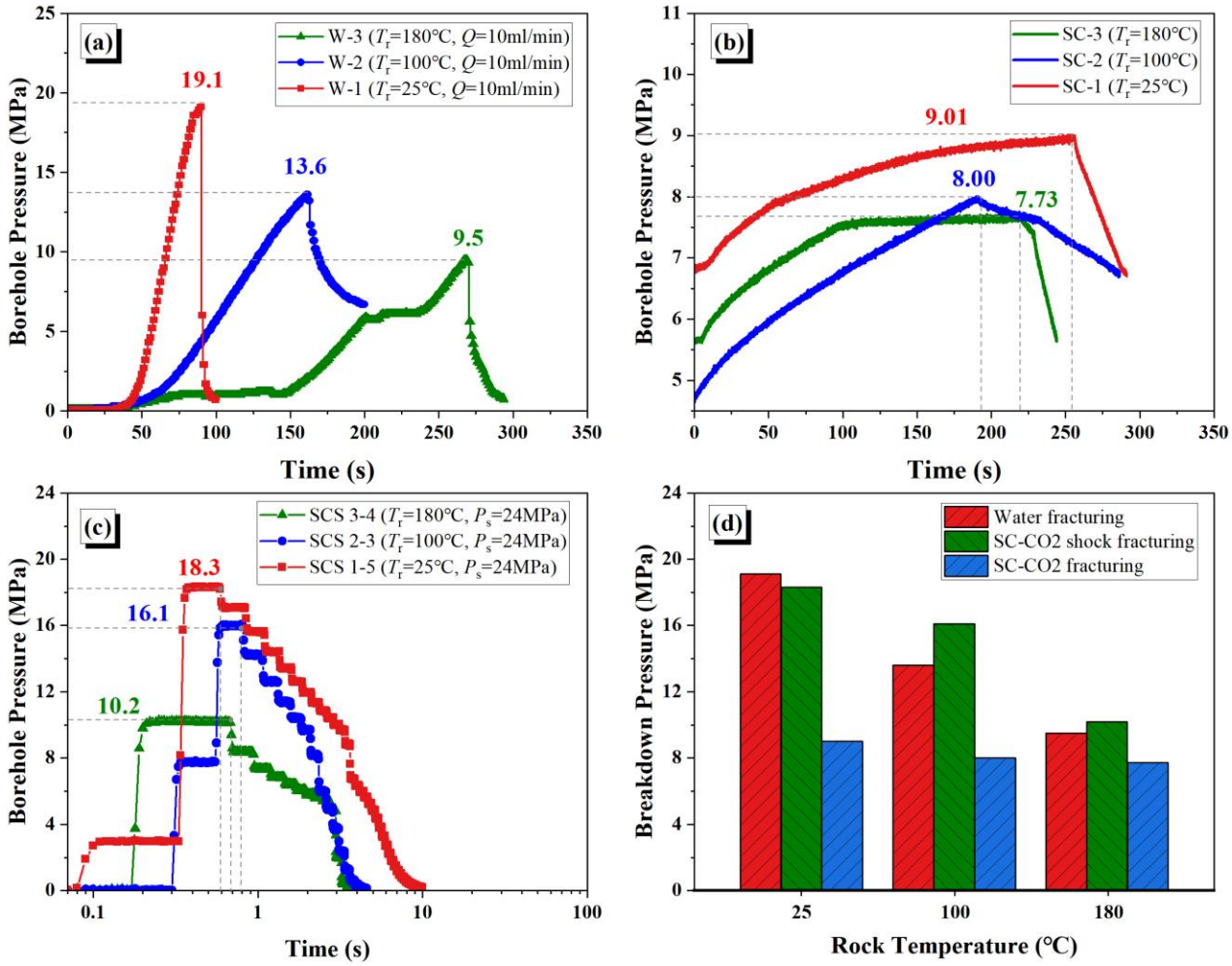

Fig. 4 Borehole pressure curves of different fracturing methods in granites with different temperatures, (a) Water fracturing; (b) SC-CO2 fracturing; (c) SC-CO2 shock fracturing with the shock pressure of 24 Mpa; (d) Comparison in the breakdown pressure between water fracturing, SC-CO2 fracturing and SC-CO2 shock fracturing. T_r represents the temperature of rock. Q represents the flow rate. P_s represents the shock pressure.

3.2 Fracture propagation pattern

Fracture propagation pattern directly determines the heat extraction volume of EGS and the connectivity between injection well and production well, which is the key to measure the effectiveness of geothermal reservoir stimulation. However, narrow fractures on the granite are sometimes not noticeable and even invisible after tests. To better identify the fracture pattern and evaluate the conductivity of the fracture networks after fracturing, we reinjected dye solution into the granite samples with a flow rate of 20ml/min in the absence of confining stress, and marked the leaking areas in blue to highlight the fracture propagation path. Fig. 5 shows the fracture patterns in granite samples subjected to SCS fracturing under different rock temperature conditions. Although the SCS fracturing is an instantaneous loading process, the rock temperature could still have a positive effect on its stimulation performance. Compared to

the granite at 25℃ as shown in Fig. 5a, high-temperature granites shown in Fig. 5b and 5c are more likely to form complex fracture networks under the same shock pressure, with more interconnected branches and larger seepage spaces created, indicating that the SCS fracturing may have a better applicability in HDR reservoirs. Furthermore, the shock pressure is an important factor influencing the fracturing pattern as well. As expected, the complexity and connectivity of fracture networks improve significantly with increasing shock pressure.

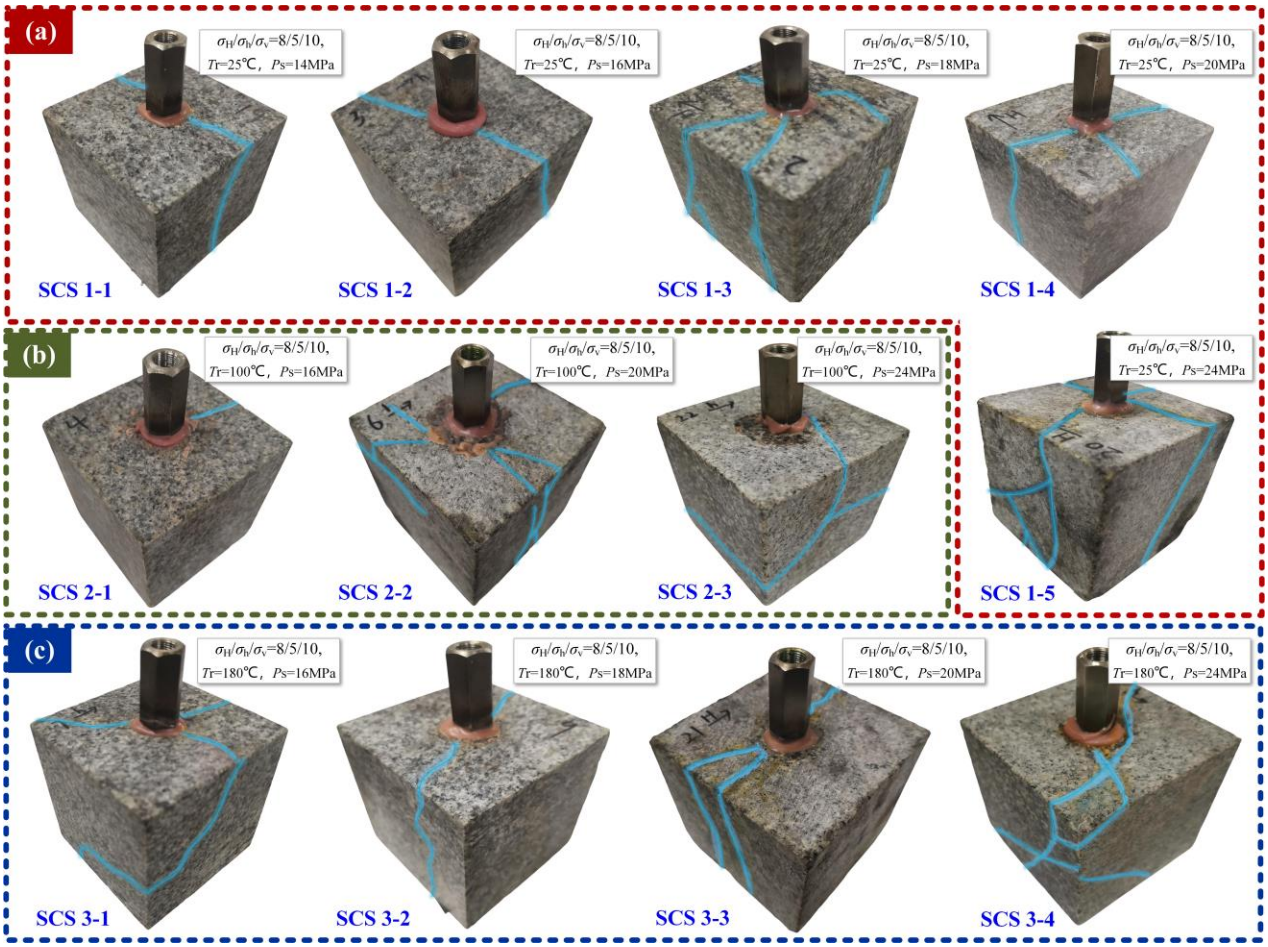

Fig. 5 SC-CO2 shock fracturing performance in granites with different temperature and shock pressure, (a) Granite samples at 25℃; (b) Granite samples at 100℃; (c) Granite samples at 180℃.

To better illuminate the feature of the fracture propagation after SCS fracturing, the fold-out diagrams showing six surfaces of the treated granite cubes at the temperature of 25, 100 and 180℃ are plotted in Fig. 6a~6c, and contrasted with those after water fracturing and SC fracturing as shown in Fig. 6d~6f and Fig. 6g~6i, respectively. The stress coordinates in these figures represents the tri-axial stress loading directions from the top view of the granite samples. By comparing different fracturing methods, it can be found that the fracture created by SCS fracturing has more branches under the same rock temperature and stress conditions, forming a fracture network with significantly higher complexity and connectivity. Unlike water fracturing and SC fracturing, SCS fracturing shows merits in getting rid of the control of in-situ stress, and the fracture can propagate in a more random direction. In addition to the direction of maximum principal stress, several fracture branches even propagate along the minimum principal stress direction in SCS fracturing as shown in Fig. 6a~6c. Moreover, rock temperature has a great influence on the tortuosity of the fracture. As the temperature of rock increases, the tortuosity of fractures improves significantly. For granite samples at 25℃, the fracture of water fracturing and SC fracturing basically propagates along the direction of maximum principal stress, resulting in a relatively straight fracture plane. Nevertheless, for granite samples at 100℃ and 180℃, the fracture deflects from the maximum principal stress direction remarkably. A more curved fracture was created under high temperature conditions, which increases the tortuosity dramatically. The complex interconnected fracture network with high tortuosity in SCS fracturing benefits to extend the flow path of working medium, enhance the heat transfer performances, and prolong the serving life of EGS in the HDR geothermal reservoir.

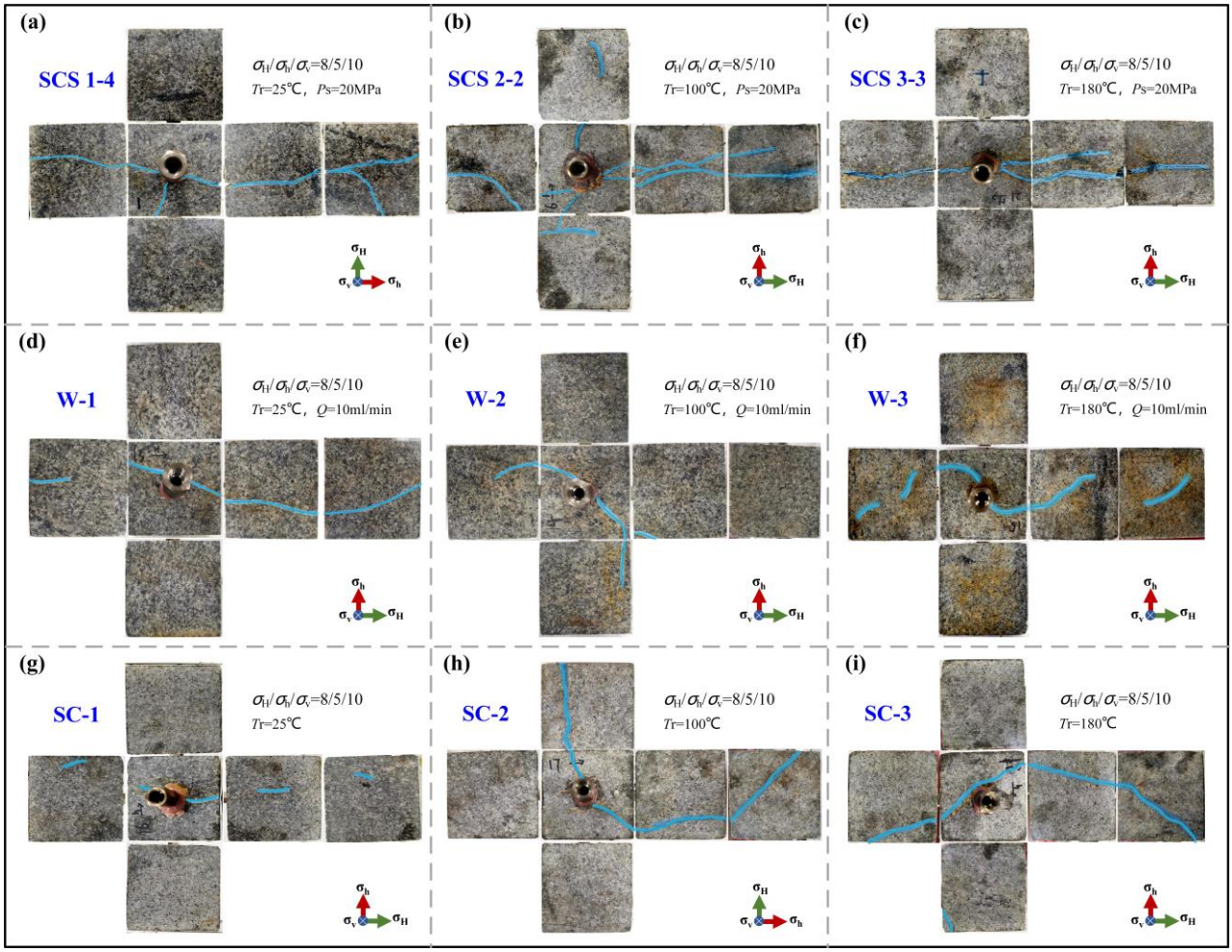

Fig. 6 Comparison in fracture patterns between various fracturing methods under different rock temperatures, (a) SC-CO2 shock fracturing of granite at 25℃; (b) SC-CO2 shock fracturing of granite at 100℃; (c) SC-CO2 shock fracturing of granite at 180℃; (d) Water fracturing of granite at 25℃; (e) Water fracturing of granite at 100℃; (f) Water fracturing of granite at 180℃; (g) SC-CO2 fracturing of granite at 25℃; (h) SC-CO2 fracturing of granite at 100℃; (i) SC-CO2 fracturing of granite at 180℃.

3.3 Conductivity of fracture network

Fracture conductivity is a measure of the property of a fracture to convey the produced fluids of the well, and is measured in terms of permeability and average fracture width. High-conductivity fracture is desirable for EGS, which allows greater flow fluxes and achieves better heat extraction performances. Herein, reinjection tests of water were performed on the fractured granite without confining stress, to calculate and compare the conductivity of the fracture networks after different fracturing. The equation for the fracture conductivity C_f in the reinjection tests is given by (yang et al., 2021):

$$C_f = \frac{25 q_w \mu \ln(\frac{r_e}{r_w})}{3\pi \Delta P_{wf}}$$

where q_w is the injection rate, ml/min; μ is the viscosity of reinjection fluid, which is water in our work, mPa·s; r_e represents the effective radius, which is the half side-length of the samples in this work, mm; r_w is the wellbore radius, mm; ΔP_{wf} is the pressure difference between the wellbore and fracture, Mpa.

The calculation results of fracture conductivity for granites subjected to different fracturing are illustrated in Fig. 7. As compared to room-temperature granites (25℃), the high-temperature granite has higher fracture conductivity for a given fracturing method. Although the SC fracturing can create more tortuous fractures, the fractures induced by the quasi-static loading mode of CO2 are relatively narrow and thereby have relatively lower conductivity. At the rock temperature of 25℃ and 100℃, the conductivity of SC fracturing is even lower than that of water fracturing. In contrast, in the SCS fracturing, a short dynamic impact pressure is applied to the granite. As a typical brittle material, rock is more prone to collapse under dynamic loading, thus SCS fracturing could generate a large-scale stimulation area with greater fracture width and higher fracture conductivity. The fracture conductivity of SCS fracturing is 3.4~7.0 times and 4.5~21.2 times higher than that of water fracturing and SC fracturing, respectively.

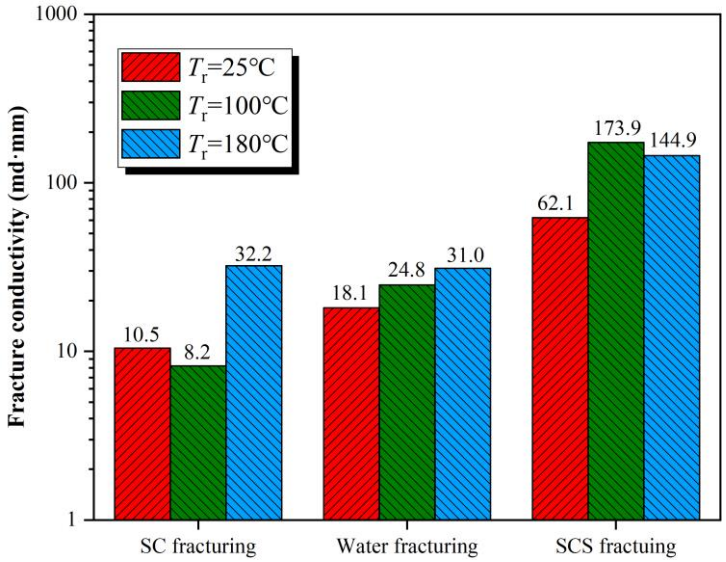

Fig. 7 Conductivity of fracture network in granites treated by different fracturing methods.

3.4 Influence of tri-axial stress conditions

In-situ stress is one of the important parameters affecting fracture morphology and complexity. The fracture propagation of traditional fracturing methods is usually significantly controlled by in-situ stress, so the fracture morphology and propagation direction are relatively simple, which characterized by single two-wing fracture. Regarding to SCS fracturing, in-situ stress plays a relatively weak role in controlling fracture propagation, unless the coefficient of horizontal stress difference is extremely high like SCS 4-1 shown in Fig. 8. Under low or moderate horizontal stress difference coefficients, such as SCS 3-3 and SCS 4-2 in Fig. 8, fracture propagation is random in direction, forming complex fractures with multiple branches. Taking the well-known FORGE site HDR geothermal reservoir as an example, the in-situ stress magnitudes in the field is σ_h=13.1~14.2 kPa/m and σ_H=13.1~14.2 kPa/m, with the coefficient of horizontal stress difference ranging in 0.08~0.41, which falls in the low to moderate level. Hence, it is possible to create complex fractures with multiple branches and high conductivity in the dry hot rock reservoir by SCS fracturing.

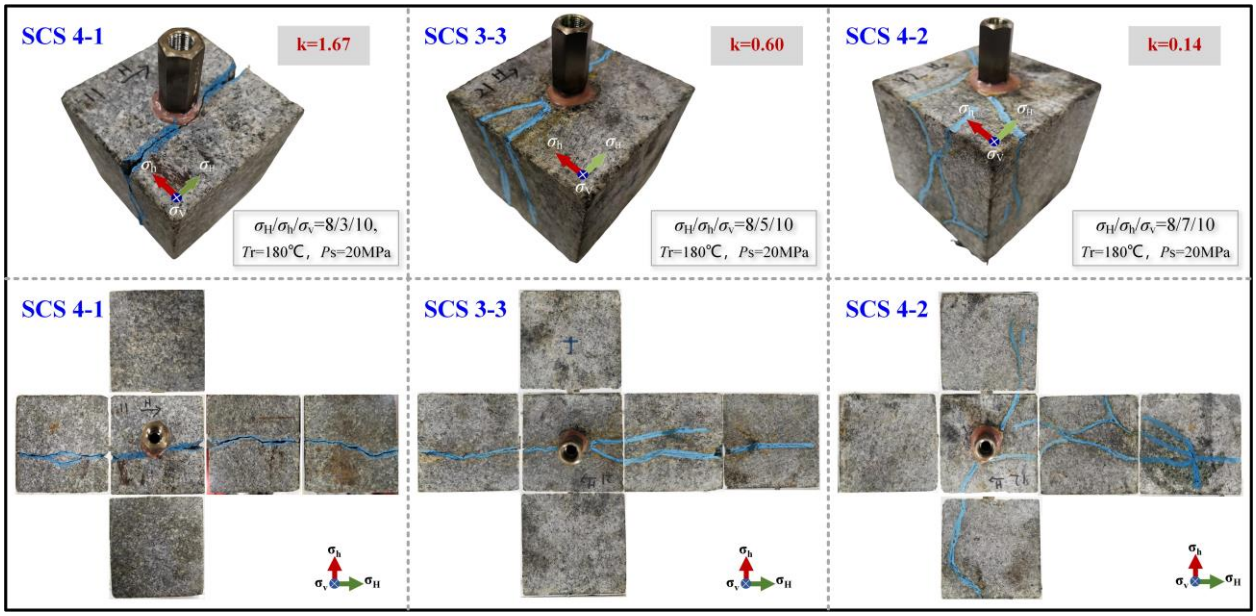

Fig. 8 Fracture patterns of granites subjected to SC-CO2 shock fracturing under different tri-axial stress conditions.

4.CONCLUSIONS

In this paper, controllable SC-CO2 shock fracturing tests were performed on high-temperature granites in a lab-scale enhanced geothermal system. By comparing with conventional water fracturing and SC-CO2 fracturing, the fracture initiation behavior and stimulation performance of SCS fracturing were determined with respect to fracture morphology and conductivity, and effects of critical parameters were investigated as well. Main conclusions are as follow:

1. The pressure evolution of SCS fracturing differs from that of water fracturing and SC fracturing greatly. Among the three fracturing methods, SC fracturing has the lowest breakdown pressure for granite samples with the same temperature, substantiating that the low-

viscosity and low-density supercritical fluid benefits to lower the breakdown pressure of granite. In the SCS fracturing, the borehole pressure reaches to the peak rapidly in hundred milliseconds, applying a dynamic load in the wellbore, and then drops to 0MPa in a stepwise manner in several seconds. The whole fracturing period is less than 10 seconds, which is significantly shorter than those of water fracturing and SC fracturing. There are multiple short pressure plateaus in the curves due to the pressure wave reflection and hedging in the borehole. The breakdown pressure is 24.2~57.5% lower than the shock pressure during SCS fracturing, and it decreases with increasing rock temperature. As compared to the granite at 25℃, the breakdown pressure of granite at 180℃ reduces by 50.3%, 14.2% and 44.3% for water fracturing, SC fracturing and SCS fracturing, respectively.

2. The fracture created by SCS fracturing has more branches under the same conditions, forming a fracture network with significantly higher complexity and connectivity. Unlike water fracturing and SC fracturing, SCS fracturing shows merits in getting rid of the control of in-situ stress, and the fracture can propagate in a more random direction. In addition to the direction of maximum principal stress, several fracture branches even propagate along the minimum principal stress direction in SCS fracturing. SCS fracturing could generate a large-scale stimulation area with greater fracture width and higher fracture conductivity. The fracture conductivity of SCS fracturing is 3.4~7.0 times and 4.5~21.2 times higher than that of water fracturing and SC fracturing, respectively.

3. Rock temperature has a positive effect on the stimulation performance of SCS fracturing. As the rock temperature increases, both the tortuosity and conductivity of fractures improve dramatically. High-temperature granites are more likely to form complex fracture networks under the same shock pressure, with more interconnected branches and larger seepage spaces created, indicating that the SCS fracturing may have a better applicability in HDR reservoirs. Although the SC fracturing can also create tortuous fractures, the fractures induced by the quasi-static loading mode of CO2 are relatively narrow and thereby have relatively lower conductivity as compared to SCS fracturing. The complex fracture network with high tortuosity and high conductivity in SCS fracturing benefits to extend the flow path of working medium, enhance the heat transfer performances, and prolong the serving life of EGS in the HDR geothermal reservoir.

4. In-situ stress is an important parameter affecting fracture morphology and complexity in SCS fracturing. The fracture propagation of conventional water fracturing is usually significantly controlled by in-situ stress, so the fracture morphology and propagation direction are relatively simple, which characterized by single two-wing fracture plane. Regarding to SCS fracturing, in-situ stress plays a relatively weak role in controlling fracture propagation. Under low or moderate horizontal stress difference coefficients (0.14~0.60), the propagation of fractures behaves more randomly in direction, contributing to forming complex fractures with multiple branches, which is desirable for the stimulation of HDR geothermal.

5. The control degree of in-situ stress on the fracture patterns is closely related to the amplitude of shock pressure in SCS fracturing. Under the conditions of low shock pressure, the fracture propagation is dominated by the in-situ stress, in which cases SCS fracturing created a typical two-wing fracture along the direction of maximum principal stress. However, as the shock pressure increases, the control of in-situ stress on fracture patterns becomes less dominant, and the number of branches and complexity of fractures improves significantly.

ACKNOWLEDGEMENT

This work was supported by national Natural Science Foundation of China (No. 52204019, No.52192624, No.52192621), the Beijing Outstanding Young Scientist Program (BJJWZYJH01201911414038), and the Science Foundation of China University of Petroleum, Beijing (No. 2462022QZDX005).

REFERENCES

Chen Y, Zhang H, Zhu Z, et al.: A new shock-wave test apparatus for liquid CO2 blasting and measurement analysis, *Measurement and Control*, 52(5-6), (2019), 399-408.

Cong R, Yang R, Wang H, et al.: Supercritical CO2 Shock Fracturing on Coal: Experimental Investigation on Fracture Morphology and Pressure Characteristics, *Proceedings*, 56th US Rock Mechanics/Geomechanics Symposium, Santa Fe, New Mexico, USA (2022).

Cui X, Ke B, Yu S, et al.: Energy characteristics of seismic waves on Cardox blasting tube, *Geofluids*, 2021, (2021), 1-13.

Huenges E.: Enhanced geothermal systems: Review and status of research and development, *Geothermal power generation*, 2016, 743-61.

Hu G, He W, Sun M.: Enhancing coal seam gas using liquid CO2 phase-transition blasting with cross-measure borehole, *Journal of Natural Gas Science and Engineering*, 60, (2018), 164-173.

Hu X, Zhang R, Zhang B, et al.: A Study on the Factors Influencing Coal Fracturing Range Caused by Liquid Carbon Dioxide Phase Transition, *Geofluids*, 2022, (2022), 4754764.

Ke B, Zhou K, Xu C, et al.: Thermodynamic properties and explosion energy analysis of carbon dioxide blasting systems, *Mining Technology*, 128(1), (2019), 39-50.

Olasolo P, Juárez M, Morales M, et al.: Enhanced geothermal systems(EGS): A review, *Renewable and Sustainable Energy Reviews*, 56, 2016, 133-44.

Pollack A, Horne R, Mukerji T.: What are the challenges in developing enhanced geothermal systems (EGS)? Observations from 64 EGS sites, *Proceedings*, World Geothermal Congress, Reykjavík, Iceland (2020).

Shi Y, Song X, Wang G, et al.: Study on wellbore fluid flow and heat transfer of a multilateral-well CO2 enhanced geothermal system, *Applied Energy*, 249, 2019, 14-27.

Shang Z, Wang H, Li B, et al.: Experimental investigation of BLEVE in liquid CO2 phase-transition blasting for enhanced coalbed methane recovery, *Fuel*, 292, 2021, 120283.

Shang Z, Wang H, Li B, et al.: Fracture processes in coal measures strata under liquid CO2 phase transition blasting, *Engineering Fracture Mechanics*, 254, 2021, 107902.

Shang Z, Wang H, Li B, et al.: The effect of leakage characteristics of liquid CO2 phase transition on fracturing coal seam: applications for enhancing coalbed methane recovery, *Fuel*, 308, 2022, 122044.

Tester J, Anderson B, Batchelor A, et al.: The future of geothermal energy, *Proceedings*, Massachusetts Institute of Technology (2006).

Wang H, Cheng Z, Zou Q, et al.: Elimination of coal and gas outburst risk of an outburst-prone coal seam using controllable liquid CO2 phase transition fracturing, *Fuel*, 284, 2021, 119091.

Wang B, Li H, Xing H, et al.: Modelling of gas-driven fracturing and fragmentation in liquid CO2 blasting using finite-discrete element method, *Engineering Analysis with Boundary Elements*, 144, 2022, 409-421.

Yang R, Hong C, Huang Z, et al.: Liquid nitrogen fracturing in boreholes under true triaxial stresses: laboratory investigation on fractures initiation and morphology, *SPE Journal*, 26(01), 2021, 135-154.

Zhang Y, Deng J, Ke B, et al.: Experimental study on explosion pressure and rock breaking characteristics under liquid carbon dioxide blasting, *Advances in Civil Engineering*, 2018.

Zhu X, Jia J, Cai Z.: Classification Method and Application of Rock Fracture Ability by Supercritical CO2 Blasting, *Shock and Vibration*, 2022, 2022, 1-11.